Quantum tunability of superlattice minibands

P. Vasilopoulos
Département de Génie Physique, Ecole Polytechnique de Montréal, Case Postale 6079, Succursale A, Montréal, Canada H3C 3A7

F. M. Peeters
Department of Physics, University of Antwerp [Universitaire Instelling Antwerpen (UIA)], Universiteitsplein 1, B-2610 Wilrijk (Antwerpen) Antwerp, Belgium

D. Aitelhabti
Département de Génie Physique, Ecole Polytechnique de Montréal, Case Postale 6079, Succursale A, Montréal, Canada H3C 3A7
(Received 24 July 1989)

We show that it is possible to control the gap between the minibands of a conventional superlattice by introducing positive potential barriers in its wells or potential wells in its barriers. An appropriate choice of the position, the width d, and the height V_d (depth V_c) of these barriers (wells), achieved by standard methods, can reduce the energy minigaps to the desired values. When these barriers are introduced at the center of the wells of the original structure, the position of the second miniband E_2 in energy space changes very little with d and/or V_d whereas that of the first miniband E_1 can change by 1 to 2 orders of magnitude. This leads to a tuning of the first miniband and of the gap E_2-E_1 and is in sharp contrast with conventional structures where both E_1 and E_2 change and a control over *both* the width and the height of the barriers is necessary for band-gap tuning. Similar results are obtained for the case of wells in the barriers. Possible applications include infrared photodetectors and tuning of the tunneling current.

I. INTRODUCTION

Superlattices have been studied extensively during the last decade especially after the advent of materials growth techniques with dimensional control close to interatomic spacing, such as molecular-beam epitaxy and metal-organic chemical-vapor deposition. Unusual electronic properties such as negative differential conductivity have been observed, and a detailed band-structure engineering has become possible.[1]

In conventional superlattices the potential profile of the conduction band is of the Kronig-Penney type with the electrons described as free particles with an effective mass $m^* \neq m_0$ (effective-mass approximation), where m_0 is the bare electron mass. This gives rise to the miniband structure.

For certain infrared (ir) applications[2] it is desirable to have only two minibands with a small energy minigap. This could be achieved by varying, for example, the width and height of the potential barriers as well as the width of the wells. To obtain small transition energies this requires small barrier heights and large well widths. Furthermore, a precise control over *both* the barrier height and well width is essential. But, wide wells are much more sensitive to electric fields than narrow wells, and for small energy minigaps dark currents will be large for large well superlattices.[3]

The present method avoids these drawbacks. Small energy separations (thus small energy minigaps) can be achieved in superlattices with narrow wells by introducing positive potential barriers (of width d and of height V_d) in the middle of its wells (of width c and of depth V_c) or potential wells in the middle of its barriers (see Fig. 1). We found that in the first case the center of the second miniband (and its width) change very little with d and/or V_d whereas the energy of the first miniband (and its width) can change by 1 order of magnitude. For certain values of V_d (V_c) and/or of d (c) the energy minigap closes; these values change when the barriers (wells) are displaced out of the center of the wells (barriers) of the original superlattice structure.

The proposed superstructure, shown in Fig. 1, can be thought of as a superlattice with a complex basis and, as will be shown below, exhibits a much richer band structure than the conventional superlattices. The only previous works for superlattices with complex basis (but with a much simpler basis than that of Fig. 1) of which we are aware are those of Refs. 3 and 4. The approximate superlattice dispersion relation of Ref. 3 is a particular limit of our exact result. The same holds for the exact (numerical) superlattice dispersion of Ref. 4. In both earlier works the tuning of the first miniband and of the energy minigap and their physical interpretation are missing.

The superlattice dispersion relation pertaining to the structure shown in Fig. 1 and its various limits are derived analytically in the next section using the transfer-matrix method. In Sec. III we present its numerical evaluation for two important cases of *biperiodic* superlattices: the positive potential barrier in the quantum well and the well in the barrier. For the case of the barriers (wells) in

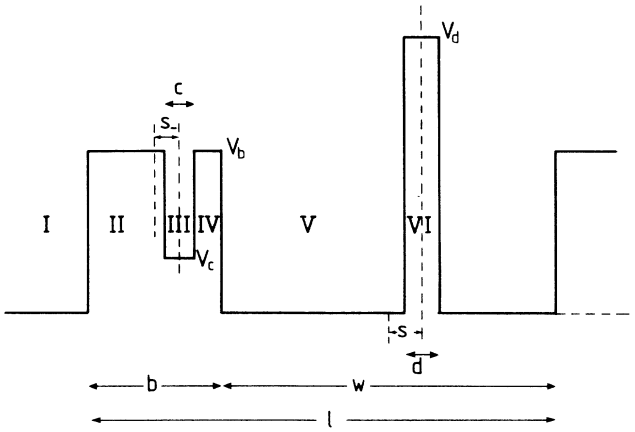

FIG. 1. Potential profile of the first period of the superlattice under investigation.

the wells (barriers) we present in the Appendix the corresponding results of an infinitely deep quantum well with a barrier or well in it. Our concluding remarks are given in Sec. IV.

II. THE DISPERSION RELATION

A. General expression

One period of the superlattice under study is shown in Fig. 1. In region I, the one-electron wave function can be written, in the effective-mass approximation, as

$$\Psi_{\rm I}(z)=A_n e^{ik(z-nl)}+B_n e^{-ik(z-nl)}\ , \tag{1}$$

and in region II as

$$\Psi_{\rm II}(z)=C_n e^{-K_b(z-nl)}+D_n e^{K_b(z-nl)}\ , \tag{2}$$

where $\hbar^2k^2=2m_w^*E$ and $\hbar^2K_b^2=2m_b^*(V_b-E)$. In regions III and V, the wave function is given by Eq. (1) with different coefficients, and the wave vector k' is defined by $\hbar^2(k')^2=2m_{w'}^*(E+V_c)$. The electron wave function in the regions IV and VI is given by Eq. (2) with decay constants K_b, for region IV, and K_d, where $\hbar^2K_d^2=2m_d^*(V_d-E)$, for region VI.

At the interfaces of the various regions we match the wave function and the quantity $(1/m^*)d\Psi/dz$ which guarantees current continuity. The matching procedure connects the coefficients A_n,B_n with A_{n+1},B_{n+1}: in matrix notation we have

$$\begin{bmatrix}A_n\\B_n\end{bmatrix}=\underline{Q}\begin{bmatrix}A_{n+1}\\B_{n+1}\end{bmatrix}\ , \tag{3}$$

which by iteration gives ($\underline{P}=\underline{Q}^{\dagger}$)

$$\begin{bmatrix}A_n\\B_n\end{bmatrix}=\underline{P}\begin{bmatrix}A_0\\B_0\end{bmatrix}\ . \tag{4}$$

The eigenvalues of $\underline{P}$ give the allowed energies (bands) and its eigenvectors the wave function, i.e., the coefficients A_0, B_0, etc. The eigenvalue equation for $\underline{P}$ is

$$p^2-{\rm Tr}\underline{P}+1=0\ . \tag{5}$$

As $n\to\pm\infty$, the wave function must remain finite, and this entails that the acceptable solutions of (5) must satisfy $|{\rm Tr}\underline{P}|\le 2$. The solutions are $p=\exp(\pm ik_z l)$ if we define $\cos(k_z l)={\rm Tr}(\underline{P})/2$. This relation gives the allowed energies (bands), i.e., the dispersion relation $E(k_z)$.

To simplify the notation for the present case, we introduce the following parameters: $\lambda_1=m_w^*/m_b^*$, $\lambda_2=m_{w'}^*/m_b$, $\lambda_3=m_w^*/m_d^*$, $r_1=\lambda_1K_b/k_w$, $r_2=\lambda_2K_b/k'$, $r_3=\lambda_3K_d/k$, $\eta_i^{\pm}=(r_i\pm 1/r_i)/2$ for $i=1,2,3$, $\eta_{ij}^{\pm}=(1/r_ir_j\pm r_ir_j)/2$ for $i,j=1,2$, $\theta_{ij}^{\pm}=(r_i/r_j\pm r_j/r_i)/2$, $\phi=ck'$, $x=(b-c)K_b$, $y=(W-d)k$, $z=dK_d$, $\rho=2s_-K_b$, and $\omega=2sk$. After a lengthy but straightforward algebraic manipulations, we obtain

$$\begin{aligned}\cos(k_z l)=&(\cos\phi\cosh x+\eta_2^-\sin\phi\sinh x)(\cos y\cosh z+\eta_3^-\sin y\sinh z)\\&+\{\eta_1^-\cos\phi\sinh x-\tfrac{1}{2}\sin\phi[(\theta_{12}^+-\eta_{12}^+)\cosh x+(\theta_{12}^++\eta_{12}^+)\cosh\rho]\}(\sin y\cosh z-\eta_3^-\cos y\sinh z)\\&+\eta_3^+\sinh z(\eta_2^+\sin\phi\sinh\rho\sin\omega+\{\eta_1^+\cos\phi\sinh x-\tfrac{1}{2}[(\theta_{12}^-+\eta_{12}^-)\cosh x+(\theta_{12}^--\eta_{12}^-)\cosh\rho]\sin\phi\}\cos\omega)\ .\end{aligned} \tag{6}$$

When narrow wells are introduced in the wells of the superlattice, in place of the narrow barriers, Eq. (6) is again valid with the interchange $K_d\to ik''$.

B. Various limits

The various limits are as follows.

(i) The standard superlattice dispersion relation is obtained from Eq. (6) for $z\to 0$ and $\phi\to 0$, i.e., when the additional barriers (K_d) and wells (k') are absent.

(ii) When only the barriers (K_d) are present (i.e., for $\phi\to 0$), we obtain

$$\begin{aligned}\cos(k_z l)=&\cosh z\cosh x\cos y\\&+(\eta_1^-\cosh z\sinh x+\eta_3^-\sinh z\cosh x)\sin y\\&+(\eta_1^+\eta_3^+\cos\omega-\eta_1^-\eta_3^-\cos y)\sinh x\sinh z\ .\end{aligned} \tag{7}$$

This expression is identical with the one we derived before[5] with the following change of notation $\eta_1^{\pm}\to\eta_b^{\pm}$ and $\eta_3^{\pm}\to\eta_d^{\pm}$. The limit of δ-function barriers of Eq. (7) is easily obtained by letting $d\to 0$ and $K_d\to 0$, while keeping the product dV_d constant. Another limit of Eq. (7) is the isolated *asymmetric* double potential well obtained for $x\to\infty$ and

$$\cosh z\cos y+(\eta_1^-\cosh z+\eta_3^-\sinh z)\sin y$$
$$+(\eta_1^+\eta_3^+\cos\omega-\eta_1^-\eta_3^-\cos y)\sinh z=0\ . \quad (8)$$

For $\eta_1^-(K_b)\to\infty$ and $\omega=0$, Eq. (8) gives the eigenvalue equation of an infinitely deep quantum well with a barrier in its center.[6] For $\eta_1^{\pm}=\eta_3^{\pm}$ and $\omega=0$, Eq. (8) gives the eigenvalue equation for the *symmetric* double-well potential.[7]

(iii) The linear *diatomic* chain limit is obtained from Eq. (7) for $K_b=K_d$ and $s=0$.

(iv) If only the wells (k') are present (i.e., for $z\to 0$), then Eq. (6) gives

$$\cos(k_z l)=(\cos\phi\cosh x+\eta_2^-\sin\phi\sinh x)\cos y+\sin y\{\eta_1^-\cos\phi\sinh x-\tfrac{1}{2}\sin\phi[(\theta_{12}^+-\eta_{12}^+)\cosh x+(\theta_{12}^+ +\eta_{12}^+)\cosh\phi]\}\ . \quad (9)$$

The δ-function limit of this expression $\phi(c)\to 0$, $V_0\to\infty$, and $cV_0\to P$ finite, gives the dispersion relation of Ref. 3 for arbitrary barrier widths b, whereas the derivation in Ref. 3 was valid only for $b\to\infty$.

(v) For $d\to\infty$ and $c\to\infty$, Eq. (7) gives the eigenvalue equation for the isolated *asymmetric* potential well.[6]

(vi) The limit of a linear *triatomic* chain is obtained for $K_b=K_d$ and $s=s_-=0$.

The list of the limits given above is not exhaustive but it indicates the richness of Eq. (6). In the following we will use Eqs. (7) and (9) and the limit of Eq. (8) for $\eta_1^-\to 0$, which gives the eigenvalue equation of an infinitely deep quantum well with a barrier in it [see Eq. (A2)].

III. NUMERICAL RESULTS

A. Positive barriers in the wells

As an example we consider $Al_xGa_{1-x}As$ barriers with $x=0.4$ (for $x>0.4$, indirect tunneling through the X valley may occur) introduced at the center of the wells of a $GaAs/Al_xGa_{1-x}As$ superlattice with $x=0.3$. The barrier heights V_d and V_b are taken to be 60% of the band-gap difference which is given[8] by $E_g=(0.093x+0.222x^2)$ eV. The effective masses are given by[8] $m^*/m_0=0.067+0.083x$. Equation (7) is solved numerically for the parameters shown in Fig. 2 in which the first two minibands are plotted as function of the barrier width d. As d increases the minibands move closer to each other and the energy minigap ΔE_g becomes smaller. Notice, however, that E_2 remains almost constant whereas E_1 has a strong dependence on d. At $d=35.9$ Å the gap closes and then reopens for $d>35.9$ Å. This is shown more clearly in Fig. 3(a) (for the same parameters as in Fig. 2), where the first two miniband widths and the gap ΔE_g are plotted as function of d. ΔE_2 remains almost constant whereas ΔE_1 changes by a factor of 5. On the other hand ΔE_g (zero at $d=35.9$ Å) increases when the barriers with a fixed width ($d=35.9$ Å) are slightly displaced from the center of the wells as shown in Fig. 3(b). Notice that

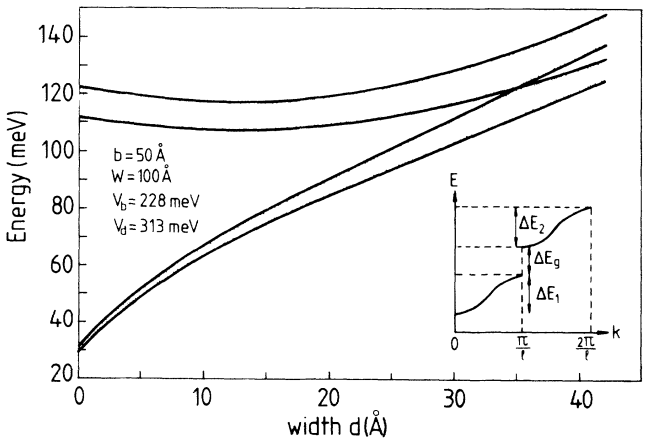

FIG. 2. The first two minibands as function of the width of the barriers placed in the middle of the quantum wells.

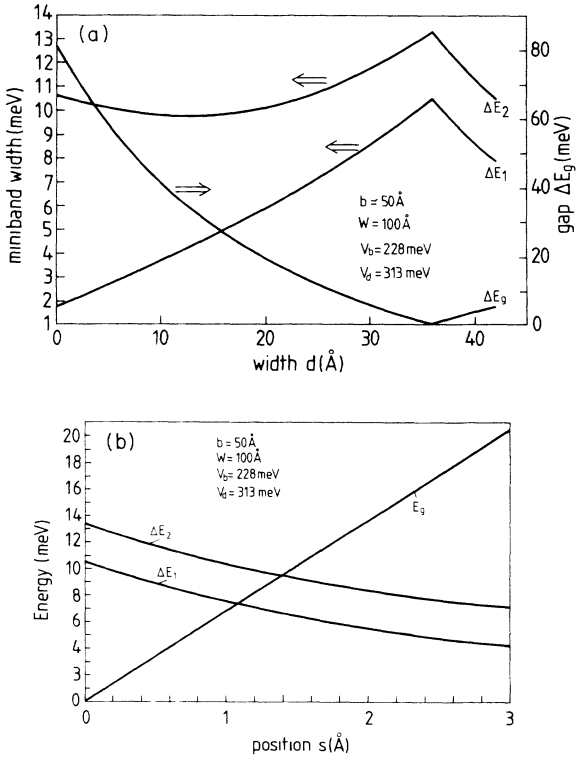

FIG. 3. (a) The width of the first two minibands and the energy gap as function of the width of the barriers which are located in the middle of the quantum wells. The dependence of these quantities on the position of the barriers with respect to the center of the quantum wells (at $s=0$ the gap is closed) is shown in (b).

when $d=0$ the gap $E_g=80.8$ meV. Inspection of Fig. 4, where $E_n(k_z)$ is plotted versus $k_z l$, shows that the second miniband has moved upwards, from its position at $d=0$ Å, by about 10 meV so that the closing of the gap is almost entirely due to the upward motion (about 90 meV) of the first miniband. In other words, varying the width of the additional $x=0.4$ barriers leads effectively to a tuning of the first miniband and of the gap since the second one remains practically constant on the meV scale. The same miniband behavior is obtained when d is fixed and V_d is varied. An additional degree of freedom is the position of these barriers (see Fig. 3). Thus for small E_2-E_1 differences, pertinent to ir applications, one does not require large wells with the disadvantages mentioned in the Introduction.

A different choice of parameters will result in different miniband widths. For example, if we take $w=200$ Å and keep all other parameters the same, the first miniband width becomes 1 order of magnitude smaller: $\Delta E_1=0.32$ meV at $d=0$ and $\Delta E_1=1.46$ meV at $d=38$ Å, when the gap closes, whereas ΔE_2 changes very little.

The previously cited miniband behavior when d or V_d is varied, especially when $s=0$, is best understood by considering the simplified model of an infinitely deep potential well with a barrier in it. This should be a good approximation especially when the barrier is placed at the center of the well. The eigenvalue equation derived along the lines of Ref. 6 or from Eq. (8) is given by Eq. (A2) of the Appendix. In Fig. 5(a) the first four energy levels are shown as function of the barrier width b for $s=0$. The other well parameters are given in the figure caption. As b increases the levels 1 and 2 (or 3 and 4) move closer to each other and for $b>50$ Å the difference E_2-E_1 is not resolved on the meV scale. Notice that it is mainly the n-odd levels that move whereas the n-even levels remain almost constant. The same behavior is obtained when b is fixed and V_0 is varied. Figure 5(b) shows how the levels move apart as s varies. This behavior is identical with that of the superlattice minibands, as shown in Figs. 2 and 3(b). We can understand this behavior with the help of Fig. 6 where the (analytically derived) wave functions $\Psi(z)$ (cf. Appendix) for the first four levels are plotted for $b=50$ Å and $s=0$ as function of z. The dashed lines are the wave functions of the first two levels in the absence of the barrier ($b=0$); the wave function of the first level has a maximum at the center of the well whereas that of the second level vanishes. Therefore, the wave function and the energy of the first level will be drastically affected by the introduction of the barrier ($b\neq 0$) whereas the corresponding quantities of the second level will not. This leads to an effective tuning of the first level and the gap E_2-E_1. This was pointed out independently for quantum wells[2(b),9] of finite height and is in direct analogy with the superlattice case as discussed above.

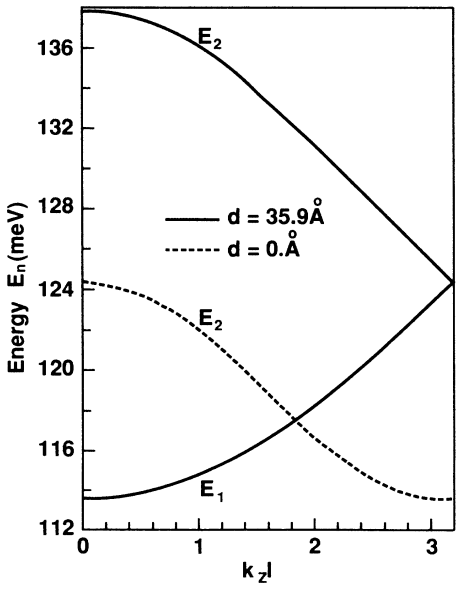

FIG. 4. The energy-momentum relation for the first two minibands for two different values of the width of the barrier. For $d=0$ Å the first miniband falls outside the figure. For $d=35.9$ Å the gap is closed.

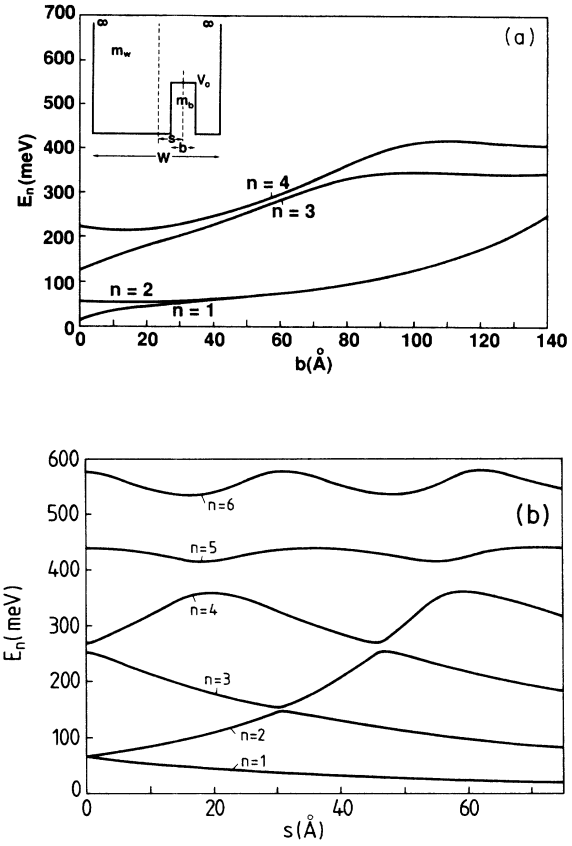

FIG. 5. (a) The first four energy levels for a potential barrier in an infinitely deep potential well (see inset) as function of the width of the barrier. In (b) the dependence of the energy levels of the potential barrier (width $b=50$ Å and height $V_0=313$ meV) in an infinitely deep well (width $w=200$ Å) is shown as function of the shift (s) of the center of the barrier from the center of the well.

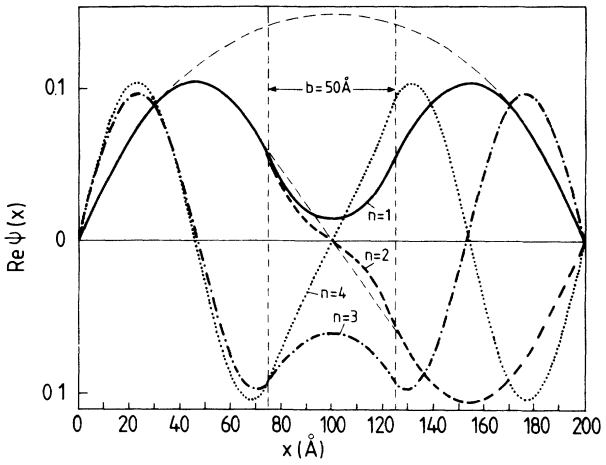

FIG. 6. The real part of the wave function corresponding to the problem of Fig. 5. The dashed thin curves correspond to the first two levels in the absence of the barrier.

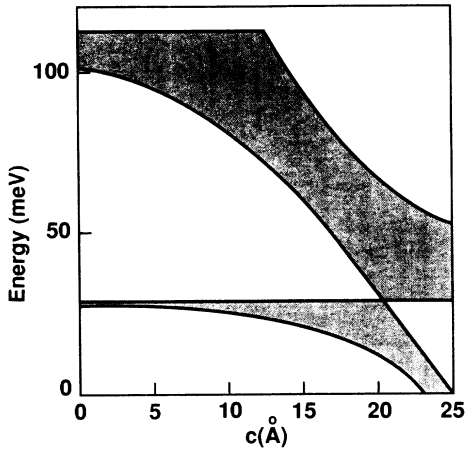

FIG. 7. The first two minibands as function of the width of the wells which are placed in the middle of the barriers. The parameters used are $b=50$ Å, $w=80$ Å, $V_b=215$ meV, and $V_c=-175$ meV.

B. Wells in the barriers

We study this case separately because when the additional wells have the same depth as the original ones, the new superlattice structure was shown to have certain advantages (lower dark current and higher responsivity[2]) over the original one. Also the δ-function limit of Eq. (9) corresponds to the case studied in Ref. 3. We consider the lattice-matched superlattice made of $Ga_{0.23}In_{0.77}As_{0.5}P_{0.5}$ wells ($m^*=0.142m_0$, $w=80$ Å) and of InP barriers ($m^*=0.053m_0$, $b=50$ Å) with quantum wells of $Ga_{0.47}In_{0.53}As$ ($m^*=0.53m_0$) introduced in the InP barriers.

In Fig. 7 the first two minibands, as resulting from the numerical evaluation of Eq. (9), are shown as function of the width c of the additional well. The other parameters used are given in the figure caption. The behavior of the minibands as function of the $Ga_xIn_{1-x}As$ well width is similar to that of Fig. 2. The gap closes at $c=20.20$ Å. The behavior of the gap and the bandwidths as function of c is shown in Fig. 8. The dispersion relation without $Ga_xIn_{1-x}As$ wells ($c=0$ dashed curves) and with those wells ($c\neq 0$ full curves) is shown in Fig. 9. Notice, however, that now it is E_1 which changes little with c whereas E_2 changes a lot. These results as well as the closing of the gap can again be understood from the behavior of the wave functions of the isolated symmetric double potential well which should be a reasonable approximation to the superlattice in the absence of the $Ga_xIn_{1-x}As$ wells. As seen in Fig. 15.5 of Ref. 7, the antisymmetric wave functions vanish in the middle of the barriers whereas the symmetric ones do not. Thus, the introduction of the additional wells in the middle of the barriers will mainly influence the symmetric wave functions.

It is of interest to study the effect of introducing impurities (donors) in the barriers of a standard superlattice which are confined to a single monolayer since this "δ doping" can lead to very-high electron densities. This was done in Ref. 3 where they used the dispersion relation which is the δ-function limit ($c\to 0$), $V_0\to\infty$, and $cV_0\to P$ finite) of Eq. (9). The behavior of the minibands observed is similar to the one described above. However, one may question the approximation of representing the effect of donors by a δ-function potential. Indeed, in Ref. 10 it was shown that the effect of such a layer gives rise to a potential of Coulomb type. We believe that Eq. (9) for narrow $Ga_xIn_{1-x}As$ wells is a better approximation to the true potential than its δ-function limit [see Eq. (1) of Ref. 3] despite the fact that the effective-mass approximation may be questionable for narrow wells.

IV. CONCLUDING REMARKS

In the present paper we have derived an analytic expression for the dispersion relation for the complex superlattice structure whose first period is depicted in Fig.

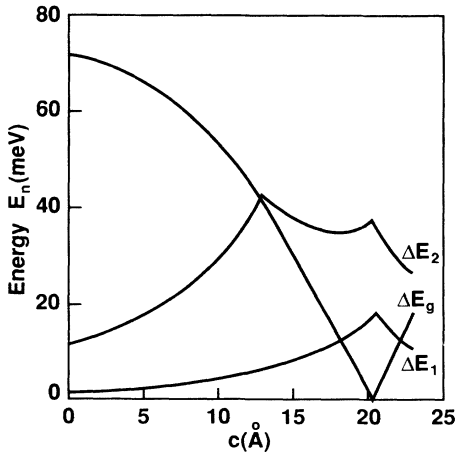

FIG. 8. The width of the first two minibands and the energy gap as function of the width of the well which is located in the middle of the barriers.

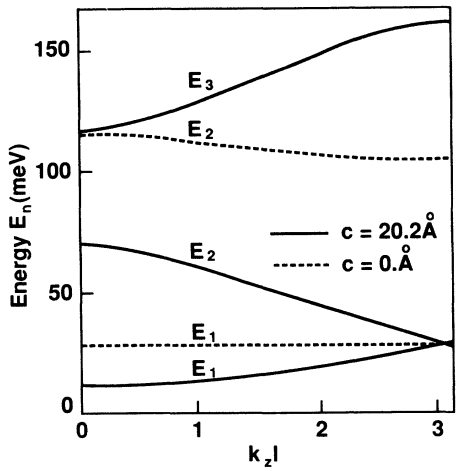

FIG. 9. The energy-momentum relation for the first three minibands for two different values of the width of the wells. For $c=0$ Å the third miniband falls outside the figure, and when $c=20.2$ Å the gap is closed.

1. The band structure as detailed in Sec. II B, Eq. (7), is very rich, and we showed how different existing results are reobtained as limiting cases. We have also presented numerical results for two important limiting cases: the one with positive potential barriers in the wells and the other with wells in the barriers of the superlattice. An important common aspect of these results is an additional freedom that one has, with respect to the conventional superlattice structures, in controlling the gap between the minibands of the superlattice (or between the levels of an isolated well, see Sec. III). The gap is easily controlled by an appropriate choice of the width, the height, and the position of the additional barriers or wells. In this way one can avoid the disadvantages of large wells mentioned in the introduction (e.g., large dark currents and strong sensitivity to the electric fields). An important point, especially in the case of barriers (see Sec. III), is that the second miniband is little affected by their presence whereas the first one is drastically affected (the reverse holds for the case of wells in barriers). This behavior and the closing of the gap is tied to that of the corresponding wave functions as approximated by those of the isolated wells (see Sec. III).

The strong sensitivity of the gap on the accuracy of centering the barrier (well) in the quantum well (barrier) [see Figs. 3 and 5(b)] may be a problem, which is also encountered in the case of positive defects in barriers discussed by Beltram and Capasso.[3] This may be compensated for by altering the height of the barriers.

The control of the gap has important applications. (1) For $V_d=V_b$ a higher responsitivity and a large reduction of the dark current in photodetectors have been reported.[2] (2) One can tune the mobility or the effective-mass ratio of the second to the first miniband.[4] (3) Since incident energies corresponding to the gap are totally reflected, the closing of the gap will lead to a higher transmittivity, e.g., a higher tunneling current [note that the group velocity, $\partial E_n(k)/\partial k$, at the point where the gap closes is not zero].

Of course other barriers (made out of different materials) may be more feasible. Higher barriers in the quantum wells will have the advantage that smaller barrier widths are needed in order to close the gap. The advantage of using $Al_xGa_{1-x}As$ barriers in a $GaAs/Al_xGa_{1-x}As$ superlattice is obvious from the grower's stand-point: only a small number of different elements are needed in the growth chamber. Similar remarks hold for the case of wells in the barriers.

In conclusion, we have proposed a new method of controlling the gap between the minibands of a superlattice. Already one particular case of the new superstructure was shown to have several advantages over the conventional structures.[2(a)] Optical experiments for the case of an isolated quantum well with a barrier in it have been reported[11] and we expect that this will be the case with the new superlattice as well. A study of plasmons in these new structures has been undertaken[12] and a study of perpendicular transport (e.g., tunneling current) has been planned.[13]

ACKNOWLEDGMENTS

This work was supported by Natural Sciences and Engineering Research Council (NSERC) of Canada Grant No. URF-35154 and by the North Atlantic Treaty Organization Collaborative Research Grant No. NATO-5-2-05/RG No.-0123/89. One of us (F.M.P.) is supported by the Belgian National Science Foundation.

APPENDIX

Below we derive the eigenvalue equation and the one-electron wave function for an infinitely deep quantum well with a barrier in it. We do so because we use them to understand the behavior of the superlattice minibands (see Sec. III) and because we did not find the relevant expressions in the literature.

In the three regions I, II, and III [see inset of Fig. 5(a)] the corresponding wave function $\Psi(z)$ can be written as

$$\Psi(z)=\begin{cases}\Psi_{\rm I}(z)=A\sin(kz), & 0\le z\le W_1\\ \Psi_{\rm II}(z)=B_1e^{K_dz}+B_2e^{-K_dz}, & W_1\le z\le W_1+d\\ \Psi_{\rm III}(z)=C\sin K(W-z), & W_1+d\le z\le W\end{cases} \tag{A1}$$

where $W_1=(W-d)/2+s$. Matching the wave function and the quantity $(1/m^*)d\Psi/dz$ at the interfaces leads to a system of four linear equations for the unknowns A, B_1, B_2, and C. The vanishing of the determinant of these coefficients gives the eigenvalue equation for $E<V_d$

$$(\alpha_1+1)(\alpha_2+1)e^{2dK_d}=(\alpha_1-1)(\alpha_2-1)\ , \tag{A2}$$

where $\alpha_1=(\lambda_3K_d/k)\tanh(kW_1)$ and $\alpha_2=(\lambda_3K_d/k)\tanh(kW_2)$ with $W_2=W-(W_1+d)=(W-d)/2-s$. Equation (A2) can also be derived from Eq. (9) for η_1^- (or K_b) $\rightarrow\infty$. The coefficients a, B_1, B_2, and C are related (through the matching procedure) by

$$\begin{aligned} C&=(\alpha_2+1)e^{dK_d}A/(\alpha_1-1)\ ,\\ B_1&=e^{-W_1K_d}(\alpha_2+1)MA\ ,\\ B_2&=e^{W_1K_d}(\alpha_2-1)MA\ , \end{aligned} \tag{A3}$$

where $M=(k/2\lambda_3K_d)\cos(kW_1)$. Normalizing the wave function in the interval $0\le z\le W$ gives

$$\begin{aligned} A=\Big\{&\tfrac{1}{2}(W_1+r^2W_2)-\frac{1}{4k}[\sin(2kW_1)+r^2\sin(2kW_2)]\\ &+4M^2\rho\sinh(dK_d)[K_d(\alpha_2^2+1)\cosh(2W_1+d)+K_d\alpha_2\sinh(2W_1+d)]+2M^2b(\alpha_2^2-1)\Big\}^{-1/2}\ , \end{aligned} \tag{A4}$$

where $r=(\alpha_2+1)e^{dK_d}/(\alpha_1-1)$. In the case of a well, of depth $-V_d$ and width d, all the results above hold with K_d replaced by ik'.

[1]R. Dingle, in *Semiconductors and Semimetals* (Academic, New York, 1987), Vol. 24.

[2](a) K. K. Choi, B. F. Levine, C. G. Bethea, J. Walker, and R. J. Malik, Phys. Rev. Lett. **59**, 2459 (1987); (b) A. Petrou and B. D. McCombe (private communication).

[3]F. Beltram and F. Capasso, Phys. Rev. B **38**, 3580 (1988).

[4]P. Yuh and K. L. Wang, Phys. Rev. B **38**, 13 307 (1988).

[5]F. M. Peeters and P. Vasilopoulos, Appl. Phys. Lett. **55**, 1106 (1989).

[6]D. Ter Haar, *Problems in Quantum Mechanics* (Infosearch, London, 1964).

[7]M. A. Morisson, T. L. Estle, and N. F. Lane, *Quantum States of Atoms, Molecules and Solids* (Prentice-Hall, New Jersey, 1976).

[8]S. Adachi, J. Appl. Phys. **58**, R1 (1985).

[9]W. Trzeciakowski and B. D. McCombe, Appl. Phys. Lett. **55**, 891 (1989).

[10]C. Mailhiot, Yia-Chung Chang, and T. C. McGill, Phys. Rev. B **26**, 4449 (1982).

[11]A. Lorke, A. D. Wieck, U. Merkt, G. Weimann, and W. Schlapp, Superlatt. Microstruct. **5**, 279 (1989).

[12]G. Gumbs (unpublished).

[13]F. M. Peeters and P. Vasilopoulos (unpublished).

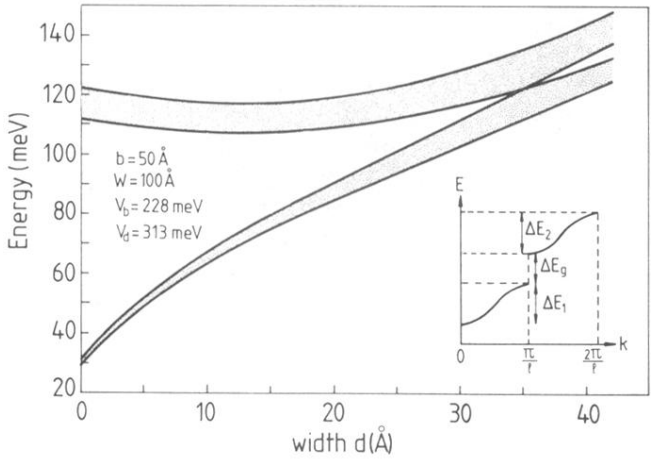

FIG. 2. The first two minibands as function of the width of the barriers placed in the middle of the quantum wells.

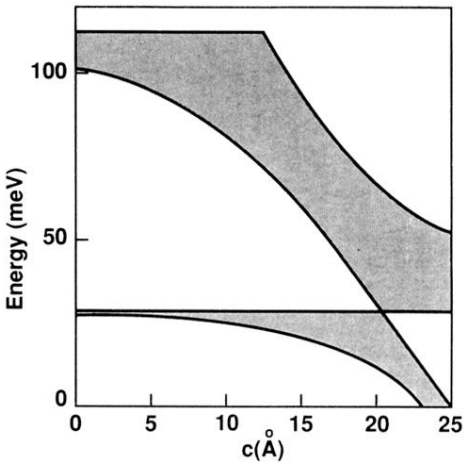

FIG. 7. The first two minibands as function of the width of the wells which are placed in the middle of the barriers. The parameters used are $b = 50$ Å, $w = 80$ Å, $V_b = 215$ meV, and $V_c = -175$ meV.